ISSN 1063-7834, Physics of the Solid State, 2015, Vol. 57, No. 2, pp. 337–343. © Pleiades Publishing, Ltd., 2015.
Original Russian Text © G.V. Garkushin, S.V. Razorenov, V.A. Krasnoveikin, A.A. Kozulin, V.A. Skripnyak, 2015, published in Fizika Tverdogo Tela, 2015, Vol. 57, No. 2, pp. 321–327.

MECHANICAL PROPERTIES, PHYSICS OF STRENGTH, AND PLASTICITY

Effect of Structural Factors on Mechanical Properties of the Magnesium Alloy Ma2-1 under Quasi-Static and High Strain Rate Deformation Conditions

G. V. Garkushin[a, b, *], S. V. Razorenov[a, b], V. A. Krasnoveikin[b], A. A. Kozulin[b], and V. A. Skripnyak[b]

[a] *Institute of Problems of Chemical Physics, Russian Academy of Sciences, pr. Akademika Semenova 1, Chernogolovka, Moscow oblast, 142432 Russia*

* *e-mail: garkushin@ficp.ac.ru*

[b] *National Research Tomsk State University, pr. Lenin 36, Tomsk, 634050 Russia*

Received July 7, 2014

Abstract—The elastic limit and tensile strength of deformed magnesium alloys Ma2-1 with different structures and textures were measured with the aim of finding a correlation between the spectrum of defects in the material and the resistance to deformation and fracture under quasi-static and dynamic loading conditions. The studies were performed using specimens in the as-received state after high-temperature annealing and specimens subjected to equal-channel angular pressing at a temperature of 250°C. The anisotropy of strength characteristics of the material after shock compression with respect to the direction of rolling of the original alloy was investigated. It was shown that, in contrast to the quasi-static loading conditions, under the shock wave loading conditions, the elastic limit and tensile strength of the magnesium alloy Ma2-1 after equal-channel angular pressing decrease as compared to the specimens in the as-received state.

DOI: 10.1134/S1063783415020109

1. INTRODUCTION

Deformable alloys of the Mg–Al–Zn–Mn system, including the magnesium alloy Ma2-1 (analog of the AZ31 alloy), have been widely used as structural materials in instrument making, aerospace, automotive, and other industries, because they have a low density at high specific strength characteristics and plasticity [1]. The mechanical properties of magnesium alloys Ma2-1 with different grained structures and textures formed during severe plastic deformation were investigated in [2–6]. The specific features of the mechanical behavior of these materials were examined predominantly under static and quasi-static loading conditions at strain rates of up to 10^3 s^{-1}. However, experimental data on the strength properties of the Ma2-1 alloy at higher strain rates are almost not available. It is known that the severe plastic deformation processing of metals and alloys not only changes the grain size and results in the formation of a texture but also generates a large amount of microscopic defects of different scale levels (dislocations, disclinations, twins, micropores, microcracks) [7]. An increase in the density of dislocations and twins leads to an increase in the resistance to plastic flow under quasi-static deformation conditions. At the same time, under severe dynamic loading conditions, the high density of microdefects can weaken the dependence of the yield strength on the strain rate. The difference in the strain rate dependences of the yield strength can be so large that, as in the case of titanium and aluminum [8], the sign of the influence of structural factors will be different upon transition from the quasi-static to dynamic loading. The relative contributions of the internal structure to the deformation resistance can be found experimentally by varying the structure of the material and the strain rate [6, 9]. In this work, we have performed comparative studies of the elastic–plastic and strength characteristics of the magnesium alloy Ma2-1 under quasi-static loading conditions at a strain rate of 10^{-3} s^{-1} and under conditions of shock wave loading of test specimens at strain rates above 10^4 s^{-1} [10].

2. MATERIALS AND EXPERIMENTAL TECHNIQUE

The test magnesium alloy Ma2-1 with the elemental composition containing 93.7% Mg, 4.36% Al, 1.34% Zn, and 0.39% Mn had the density of 1.79 g/cm^3. The experiments were performed with specimens of the Ma2-1 alloy in the coarse-grained (as-received) and fine-grained states. For all the investigations performed in this work, specimens were cut using the electric discharge machining process from an industrial rod with a diameter of 60 mm. The texture and grain size of the magnesium alloy specimens were changed using multipass equal-channel angular pressing with orthogonal channels [7]. Since the

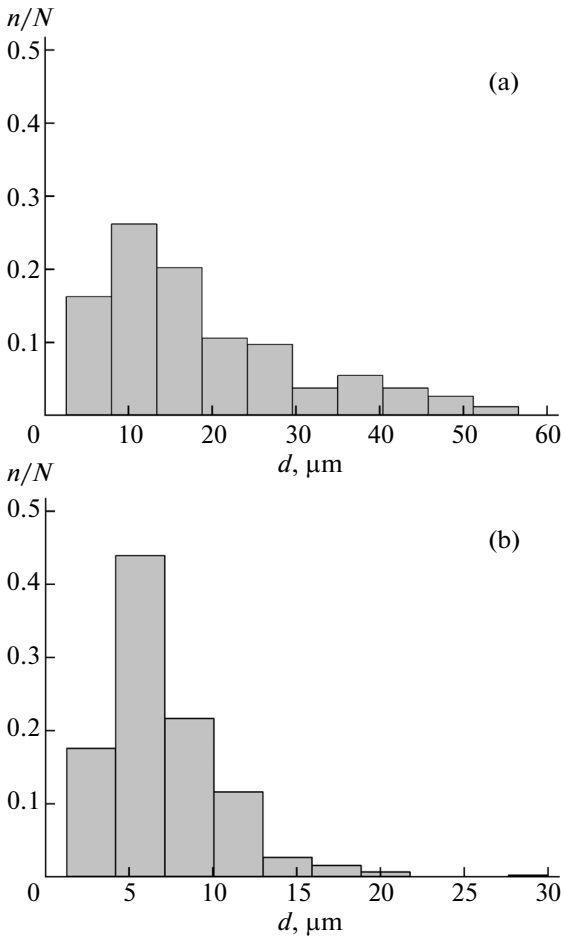

Fig. 1. Histograms of grain size distributions in the magnesium alloy Ma2-1: (a) in the as-received state and (b) after equal-channel angular pressing.

deformed magnesium alloy Ma2-1 with a sufficiently high strength had a low ductility at temperatures below 200°C, the equal-channel angular pressing was carried out at a temperature of 250 ± 2°C. Traditional methods of deformation of alloys (rolling, extrusion, compression molding, and others.) make it possible to decrease the average size of grains to the micrometer level, but cannot change the type of basic texture that inhibits the activity of the basic and other types of slip [3].

The equal-channel angular pressing of the specimens was performed using counter-pressure. Each cycle along the route B_c at the given temperature included the extrusion of a block through a channel of constant cross section with the rotation of the workpiece by 90° around the longitudinal axis up to four times. The microstructural analysis of the initial specimens demonstrated that the magnesium alloy Ma2-1 in the as-received state had grain sizes ranging from 2 to 55 μm. After the equal-channel angular pressing at a temperature of 250°C, the grain refinement was observed in the Ma2-1 alloy due to the severe plastic deformation and dynamic recrystallization. Under the chosen conditions, the pressing of the specimen resulted in the formation of a homogeneous grain–subgrain structure with an average grain size of 7 μm. It should be noted that, after the equal-channel angular pressing, the structure of the Ma2-1 alloy contained single coarse grains with sizes of ~15–30 μm, which were not undergone refinement. Figures 1a and 1b show the histograms of the grain size distributions, where d is the grain size.

The Rockwell hardness of the test specimens was determined on a Rockwell Hardness Tester TH300 using a steel indenter with a diameter of 1.6 mm, a strength of 60 kgF, and an exposure time of 3 s. The hardness of the alloy specimens in the as-received state was equal to 61 ± 2 HRF, whereas the hardness after the equal-channel angular pressing was 78 ± 3 HRF. A change in the number of equal-channel angular pressing passes from one to four weakly affected the hardness of the specimens.

The strength properties of the Ma2-1 alloy under quasi-static axial tension conditions were investigated on an INSTRON 5948 electromechanical testing machine at a strain rate of 10^{-3} s^{-1}. For tensile testing, specimens in the form of two-sided flat blades were cut using the electric discharge machining process from the material in the initial state and from specimens subjected to multipass equal-channel angular pressing along their axis. The working part of the specimens had the size of 5 × 1.2 × 10 mm.

In the experiments, the high strain rates were achieved by loading specimens with plane shock waves generated by an impact with aluminum impactor plates accelerated by an explosive device to velocities of 630 ± 30 m/s [10]. The velocity of the free rear surface of the specimen during testing was continuously measured using a VISAR laser Doppler velocimeter [11, 12]. The free-surface velocity profiles $u_{fs}(t)$ were recorded with a time resolution of ~1 ns and a velocity resolution of ±3 m/s. All the tests were performed at room temperature.

3. RESULTS AND DISCUSSION

Figure 2 shows the stress–engineering strain (σ–$\Delta l/l_0$) curves obtained from uniaxial tensile tests of the specimens of the Ma2-1 alloy in the as-received state and after two and four passes of equal-channel angular pressing along the route B_c. The results of these experiments demonstrate that, with a decrease in the grain size and upon the formation of a defect structure, the yield strength of the studied alloy increases from 150 to 200 MPa, the short-term tensile strength increases from 250 to 295 MPa, and the ultimate strain to failure of the specimens after the equal-channel angular pressing increases from 17.5 to 24%. The table presents the strength characteristics obtained by the processing of the quasi-static tensile data.

In [3], it was noted that, for a similar alloy upon the transition from the initial state to the state after the equal-channel angular extrusion on an INSTRON-1163 machine, the yield strength decreases from 220 to 132 MPa and the tensile strength decreases from 279 to 245 MPa with an increase in the uniform tensile strain. For the extruded magnesium alloy AZ31 studied in [6], it was shown that the ratio and volume distribution of small and large grains in a grained structure can have significantly different (qualitative) influences on the resistance to plastic deformation of magnesium alloys. It was noted that different equal-channel angular extrusion routes (A_c, B_c, E, etc.) lead to different textures and different volume distributions of large and small grains in the bulk of the material after the equal-channel angular extrusion. As a result, the yield strength can remain unchanged, whereas the ultimate strain to failure can increase several times. For a different texture and a different grain distribution, on the contrary, the yield strength and tensile strength increase, whereas the ultimate strain to failure decreases. The equal-channel angular pressing along the route B_c provides the formation of grained structures with a size distribution that ensures an increase in both strength characteristics, i.e., the tensile strength and the yield strength, as well as an increase in the ultimate strains. It is known that the presence of large grains or the formation of bimodal grained structures in fine-grained alloys leads to a significant increase in the ductility of ultrafine-grained alloys [7]. The discrepancy between the results obtained in this work and in [3] can be associated both with the differences in the original textures and structures of the magnesium alloys used in the works and with the difference in the equal-channel angular pressing technologies of preparation of specimens.

In order to verify the hypothesis of a possible difference in the dependences of the flow stress on the strain rate of the magnesium alloys in the coarse-grained and fine-grained states upon the transition from the quasi-static loading to the high strain rate loading, as was observed in the case of titanium and aluminum [8], we performed experiments on their shock compression. In all the shock wave compression experiments, the specimens were brought into a stress state close to the hydrostatic stress state under uniform deformation by means of their loading with plane shock waves [10]. The maximum amplitude of the shock waves in most of the experiments did not exceed ~4 GPa.

In the first series of shock wave compression experiments, the influence of high-temperature heating on the elastic–plastic characteristics of the magnesium alloy in the as-received state was estimated by comparing the strength characteristics of the specimen in the initial and annealed states. The specimens of the magnesium alloy Ma2-1 were subjected to preliminary severe plastic deformation using the equal-channel angular pressing at a temperature of 250°C, which

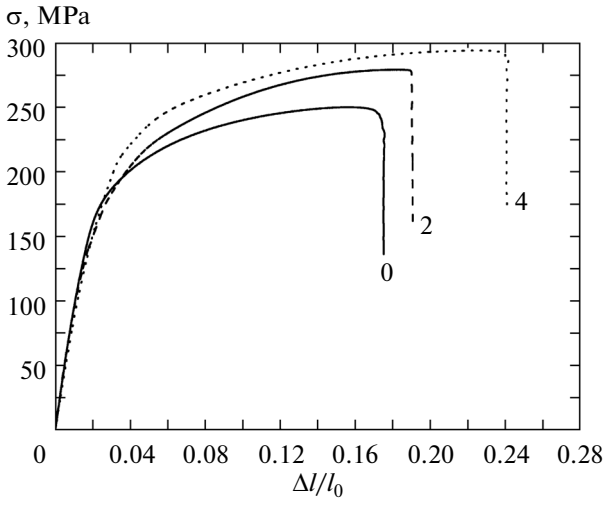

Fig. 2. Results of uniaxial tensile tests on flat specimens of the Ma2-1 alloy. Numerals near the curves indicate the number of equal-channel angular pressing passes.

could lead to annealing of the alloy. In turn, the annealing could remove residual internal stresses of the initial specimen. In our previous study [9] of the aluminum alloy D16T, we noted the strong effect of annealing, which led to an approximately twofold drop in the hardness and to a decrease in the dynamic yield strength by a factor of four to five. The preliminary annealing of the magnesium alloy specimens was performed at a temperature of 450°C for 20 min. The measurements of the hardness of the specimens before and after annealing revealed that the heat treatment did not have any effect; in both cases, the hardness was equal to 61 ± 2 HRF.

Figure 3 shows the time dependences of the free-surface velocity measured for the unannealed (dashed line) and annealed (solid line) flat specimens of the magnesium alloy in the as-received state. The wave profiles demonstrate that an elastoplastic shock compression wave and a part of the subsequent rarefaction wave appear on the surface. For the chosen ratio between the thicknesses of the impactor plate and the specimen, the loading conditions in the vicinity of the free rear surface of the specimen correspond to the

Mechanical properties of the Ma2-1 alloy before and after the equal-channel angular pressing processing

State of specimens	Yield strength, MPa	Short-term tensile strength, MPa
Initial state	150 ± 5	250 ± 10
After two equal-channel angular pressing passes	160 ± 5	280 ± 10
After four equal-channel angular pressing passes	200 ± 5	295 ± 10

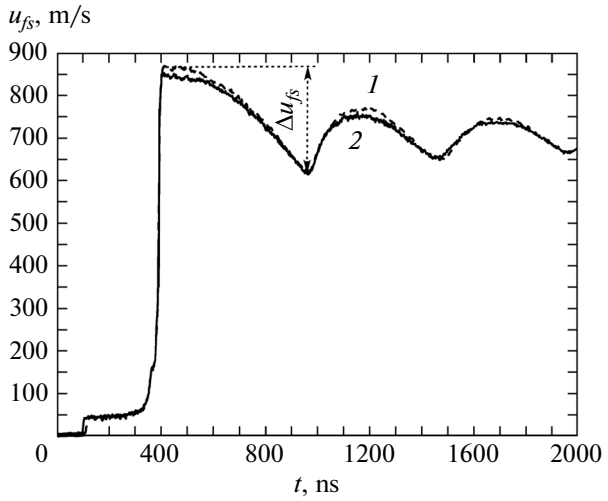

Fig. 3. Results of measurements of the free-surface velocity profiles of (*1*) annealed and (*2*) unannealed specimens of the magnesium alloy. The thicknesses of the flat specimens are 9.84 and 10.78 mm. The loading of the specimens was performed by an impact with a 2-mm-thick aluminum plate at a velocity of 630 ± 30 m/s.

onset of attenuation of the shock wave under the action of the overtaking rarefaction wave. After the reflection of the compression pulse from the free surface, tensile stresses are generated inside the specimen, which, in turn, initiates its fracture, i.e., a spall. This is accompanied by the relaxation of tensile stresses and the formation of a compression wave (spall pulse), which comes to the surface of the specimen and causes the second increase of its velocity. A further decay of oscillations of the velocity is related to the reverberation of the spall pulse in the "spall plate" detached from the specimen. The presence of an additional step at the plastic shock wave front (at the level of 160 m/s) is due to the rereflection of the elastic precursor between the free surface and the plastic shock wave.

The uniaxial compression stress behind the front of the elastic precursor, which is equal to the dynamic (Hugoniot) elastic limit of the material, can be calculated according to the formula [10]

$$\sigma_{\mathrm{HEL}} = \rho_0 c_l u_{fs}^{\mathrm{HEL}}/2, \qquad (1)$$

where ρ_0 is the density of the alloy, c_l is the longitudinal speed of sound, and u_{fs}^{HEL} is the free-surface velocity behind the front of the elastic precursor. The free-surface velocity decrement Δu_{fs} (Fig. 3), when the free-surface velocity decreases from the maximum to the value before the front of the spall pulse, is proportional to the fracture stress, i.e., the spall strength of the material under the given loading conditions. In the linear (acoustic) approximation, the spall strength has the form

$$\sigma_{sp} = \frac{1}{2}\rho_0 c_b(\Delta u_{fs} + \delta u), \qquad (2)$$

where c_b is the bulk speed of sound and δu is the correction for distortion of the wave profile due to the differences between the velocities of the spall pulse front and the velocity of the plastic part of the incident unloading wave before this front [13]. Similar distortions occur when the relaxation of stresses during fracture of a stretched material generates a compression wave whose front represents an elastic wave overtaking the unloading part of the incident compression pulse, which moves with the bulk speed of sound (c_b). The obtained results demonstrate that the preliminary annealing did not affect the character of the elastic–plastic transition and the Hugoniot elastic limit, whereas the spall strength slightly decreased from 1.04 to 1.02 GPa.

At a maximum shock compression pressure, the free-surface velocity profiles of the magnesium alloy exhibit weak irregular oscillations. Similar oscillations of the free-surface velocity can be caused by the deformation twinning in a shock compression wave under maximum compression [14, 15]. In our recent study [15], we observed similar oscillations for magnesium single crystals in the [0001] direction. The performed microstructural investigations of magnesium(0001) single-crystal specimens after the preliminary shock compression revealed intensive pyramidal twinning in the structure of the single crystals [15].

It is known that the twinning is the main mechanism of hardening under shock compression, and the concentration of twins in the bulk of the material increases with increasing pressure [16]. The twinning leads to a significant hardening of magnesium crystals [14]. In order to evaluate how the intensity of shock compression affects the resistance of the magnesium alloy to dynamic fracture, we carried out additional measurements of the spall strength of the annealed specimen in the as-received state with a thickness of 8.98 mm under loading by an impact with a 2-mm-thick aluminum plate at a velocity of 1.8 km/s. According to these measurements, the measured spall strength at a shock compression pressure of ~12.5 GPa is equal to 1.12 GPa, which is 8% higher than the spall strength measured at an impact velocity of 630 ± 30 m/s when the maximum amplitude of the shock wave is 3.8 GPa.

As is known, the original texture of the material produced by different technological methods (rolling, extrusion, heat treatment, etc.) has an influence on the resistance to deformation and fracture of the material [6, 9]. In order to elucidate the influence of the texture of the magnesium alloy specimen in the as-received state on the character of the dynamic deformation and fracture, we carried out experiments in

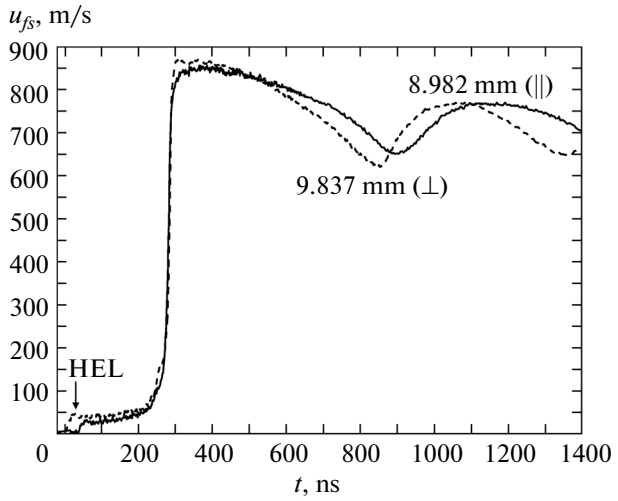

Fig. 4. Free-surface velocity profiles of the specimen of the magnesium alloy Ma2-1 in the as-received state after shock wave loading in the direction of rolling and in the transverse direction. The numbers near the curves are the thicknesses of the specimens.

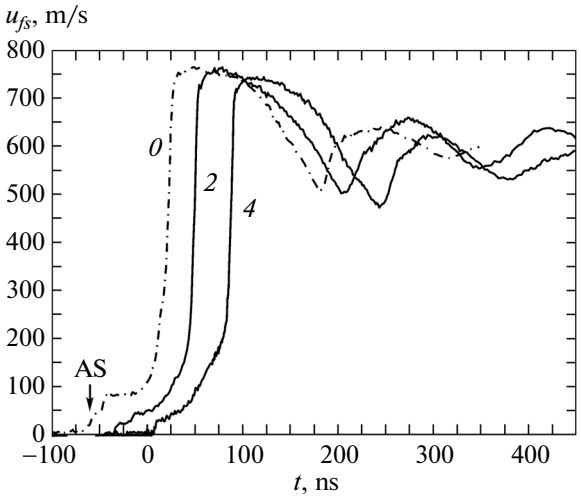

Fig. 5. Free-surface velocity profiles of the alloy specimens after (*0*) annealing, (*2*) two equal-channel angular pressing passes, and (*4*) four equal-channel angular pressing passes.

which the direction of the shock compression was varied with respect to the direction of rolling. The results of measurements of the free-surface velocity profiles of the annealed specimens of the Ma2-1 alloy in the as-received state are presented in Fig. 4. The shock wave loading was performed in the direction of rolling (||) and in the transverse direction (⊥) with the use of 2-mm-thick aluminum impactor plates at an impact velocity of 630 ± 30 m/s. A direct comparison of the free-surface velocity profiles shows that the spall strength of the specimens in the second case is approximately 17% less than the value obtained in the first case when the spall strength was equal to 1.04 GPa. In this respect, the behavior of the magnesium alloy Ma2-1 is similar to the behavior of the textured steels and aluminum alloy D16T previously studied under the same conditions [9, 17–20]. The difference we observe in the spall strengths for different orientations of the shock wave loading with respect to the direction of rolling is probably a consequence of the fact that the potential sources of fracture have an elongated shape and are oriented in the direction of rolling. The analysis of the results obtained in these experiments revealed that the texture of the Ma2-1 alloy can have an influence on the Hugoniot elastic limit. In the case of the shock wave loading in the direction perpendicular to the direction of rolling, the Hugoniot elastic limit of the Ma2-1 alloy was found to be σ_{HEL} = 215 MPa, which is ~36% higher than the Hugoniot elastic limit of the specimens loaded in the direction of rolling. As is known, the macroscopic plastic deformation in homogeneous media occurs through shifts in the directions oriented at angles close to 45° with respect to the principal axes (in our case, with respect to the compression direction). The difference between the conditions of uniaxial compression in the direction of rolling and in the transverse direction lies in the fact that, in the first case, all the shifts occur at an angle of 45° with respect to the texture fibers, whereas in the second case, a part of the shifts should occur through the displacement of the texture fibers with respect to each other. Slightly higher values obtained for the Hugoniot elastic limit of the alloy under shock compression in the direction perpendicular to the direction of rolling indicate that the displacement of the texture fibers with respect to each other under high strain rate deformation is hindered and requires the application of higher stresses [9].

Figure 5 shows the free-surface velocity profiles of the annealed specimens after two and four passes of equal-channel angular pressing of the Ma2-1 alloy. The thickness of all the specimens was ~2 mm. The loading was performed by an impact with a 0.4-mm-thick aluminum plate at a velocity of 630 ± 30 m/s. The free-surface velocity profiles shown in Fig. 5 demonstrate that there is a weak compression wave before the front of the elastic precursor (denoted as AS in Fig. 5), which is generated by an air shock wave formed before the flying impactor plate and acting on the specimen. The change in the grain size and texture due to the equal-channel angular pressing led to a decrease in the Hugoniot elastic limit of the material from 410 MPa (line *0* in Fig. 5) to 220 MPa and had no noticeable effect on the spall strength. A comparison of the free-surface velocity profiles shows that an increase in the number of equal-channel angular pressing passes from two to four does not affect the character of the elastic–plastic deformation and fracture. It was expected that the change in the texture and grain size of the magnesium specimens by means of the equal-channel angular pressing should lead to an increase in the mechanical characteristics of the alloy

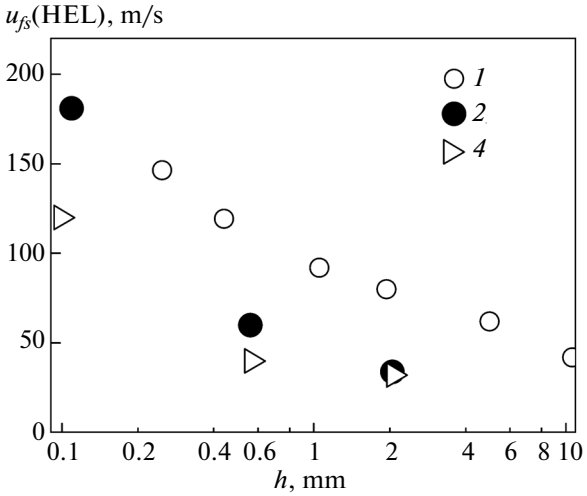

Fig. 6. Dependence of the Hugoniot elastic limit on the thickness of the test specimen of the magnesium alloy Ma2-1 according to the data obtained in (*1*) [22]; (*2*) this work, after two equal-channel angular pressing passes; and (*4*) this work, after four equal-channel angular pressing passes.

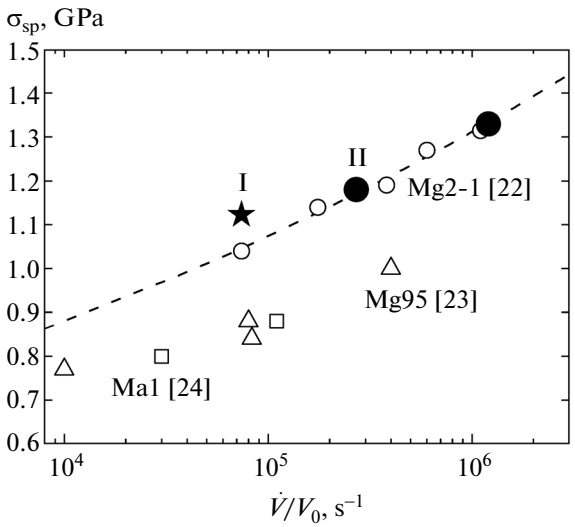

Fig. 7. Results of measurements of the spall strength of magnesium and magnesium alloys as a function of the strain rate $\dot{V}/V_0$ in a rarefaction wave according to the data obtained in this work and in [22–24].

as compared to the initial undeformed specimens, which was observed in the case of quasi-static deformation. It should be noted that the maximum hardness was observed for the fine-grained specimens of the magnesium alloy. In [21], it was noted that changes in the structure of the material did not affect the elastic–plastic characteristics of fine-grained tantalum specimens as compared to the initial specimens, whereas the hardness of tantalum increased by approximately 30%.

The results of measurements of the Hugoniot elastic limit of the magnesium alloy specimens in the as-received state [22] and in the fine-grained state are presented in Fig. 6. The maximum values of the Hugoniot elastic limit were observed for the specimens in the initial state. In [3], it was noted that, for hexagonal close-packed metals, the observed decrease in the Hugoniot elastic limit can be caused by a radical change in the texture of the material due to large shear strains, which predominantly occur in the planes inclined at an angle of 45°–50° with respect to the direction of pressing, as well as due to the dynamic recrystallization. After the equal-channel angular pressing at a temperature of 250°C, the grain refinement occurred in the Ma2-1 alloy. In this case, grains had orientations typical of those inclined to the direction of pressing by 40°–50° basic poles. In [3], it was assumed that the plastic deformation of the studied alloy under uniaxial tension at room temperature after different states is provided by the basic (0001) and prismatic dislocation slip along the $\langle 1120 \rangle$ direction, the pyramidal $\langle 1122 \rangle$ dislocation slip along the $\langle 1123 \rangle$ direction, and the twinning $(1012)\langle 1011 \rangle$. The results obtained in this study demonstrate that the orientation factor and, hence, the initial critical shear stresses for the basic slip in this alloy decrease after the equal-channel angular pressing.

The dependence of the fracture stress during spalling the Ma2-1 alloy on the strain rate is shown in Fig. 7. The rate of volumetric strain is considered to mean the rate of expansion of matter in a rarefaction wave, which is determined as

$$\frac{\dot{V}}{V_0} = -\frac{\dot{u}_{fsr}}{2c_b}, \tag{3}$$

where $\dot{u}_{fsr}$ is the measured rate of decrease in the free-surface velocity of the test specimen in the unloading part of the shock compression pulse. In Fig. 7, the asterisk (I) indicates the spall strength obtained for the Ma2-1 alloy at the impactor velocity of 1.8 km/s and the closed circles (II) denote the average spall strengths of fine-grained specimens measured after two and four equal-channel angular pressing passes. For comparison, Fig. 7 shows the previously measured spall strengths of the coarse-grained cast magnesium Mg95 [23] and the sheet magnesium Ma1 [24]. As can be seen from this figure, the spall strength of the magnesium alloy specimens after equal-channel angular pressing coincides with the data on the spall strength obtained earlier in [22] for the magnesium alloy Ma2-1 in the as-received state; i.e., the severe plastic deformation has no significant effect on the resistance to spall fracture.

4. CONCLUSIONS

In this paper, we presented new results of measurements of the quasi-static yield strength, dynamic yield strength, and dynamic tensile strength of the magnesium alloy Ma2-1 in the as-received state after high-temperature annealing and the alloy specimens subjected to severe plastic deformation using the equal-channel angular pressing along the route B_c at a temperature of 250°C. The influence of the direction of shock loading with respect to the texture of the material on the Hugoniot elastic limit and spall strength was investigated. It was found that, in the case where the direction of shock wave loading is oriented parallel to the direction of rolling, the resistance to submicrosecond fracture of the Ma2-1 alloy is less than that after the shock compression in the direction of rolling. The preliminary annealing of the alloy does not affect the character of the high strain rate deformation.

The conventional yield strength and tensile strength of the magnesium alloy Ma2-1 subjected to quasi-static loading increase as a result of the change in the structure of the material after multipass equal-channel angular pressing. After the shock wave loading, the changes observed in the grain size and texture of the material due to multipass equal-channel angular pressing lead to a decrease in the Hugoniot elastic limit and have no significant effect on the spall strength. In this case, the number of equal-channel angular pressing passes almost does not affect the strength properties of the material.

ACKNOWLEDGMENTS

We would like to thank L.G. Ermolov for the assistance in performing explosive experiments.

This study was supported by the Russian Foundation for Basic Research (project no. 12-02-31682), the Council on Grants from the President of the Russian Federation (grant no. MK-3066.2012.8), the Presidium of the Russian Academy of Sciences within the framework of the Basic Research Program 2P "High Energy Density Materials," and the National Research Tomsk State University within the framework of the International Competitiveness and Staff Capacity Enhancement Program.

REFERENCES

1. *Magnetic Alloys*, Part 1: *A Reference Book: Technology of Production and Properties of Castings and Deformed Semi-Finished Products*, Ed. by I. I. Gur'ev and M. V. Chukhrov (Metallurgiya, Moscow, 1978) [in Russian].
2. V. N. Serebryany, T. M. Ivanova, V. I. Kopylov, S. V. Dobatkin, N. N. Pozdnyakova, V. A. Pimenov, and T. I. Savelova, Russ. Metall. **2010** (7), 648 (2010).
3. V. N. Serebryanyi, G. S. D'yakonov, V. I. Kopylov, G. A. Salishchev, and S. V. Dobatkin, Phys. Met. Metallogr. **114** (5), 448 (2013).
4. V. N. Serebryanyi, S. V. Dobatkin, and V. I. Kopylov, Tekhnol. Legkikh Splavov **3**, 28 (2009).
5. F. Zhao, Y. Li, T. Suo, W. Huang, and J. Liu, Trans. Nonferrous Met. Soc. China **20**, 1316 (2010).
6. G. Wan, B. L. Wu, Y. D. Zhang, G. Y. Sha, and C. Esling, Mater. Sci. Eng., A **527,** 2915 (2010).
7. R. Z. Valiev and I. V. Aleksandrov, *Bulk Nanostructured Metal Materials: Preparation, Structure, and Properties* (Akademkniga, Moscow, 2007) [in Russian].
8. G. I. Kanel', S. V. Razorenov, A. S. Savinykh, E. B. Zaretskii, and Yu. R. Kolobov, Preprint No. 1-478, OIVT RAN (Joint Institute for High Temperatures, Russian Academy of Sciences, Moscow, 2004).
9. G. V. Garkushin, S. V. Razorenov, and G. I. Kanel', Tech. Phys. **53** (11), 1441 (2008).
10. G. I. Kanel', S. V. Razorenov, A. V. Utkin, and V. E. Fortov, *Shock-Wave Phenomena in Condensed Media* (Yanus-K, Moscow, 1996) [in Russian].
11. L. M. Barker and R. E. Hollenbach, J. Appl. Phys. **43** (11), 4669 (1972).
12. T. Antoun, L. Ceaman, D. R. Curran, G. I. Kanel, S. V. Razorenov, and A. V. Utkin, *Spall Fracture* (Springer, New York, 2003).
13. G. I. Kanel', Prikl. Mekh. Tekh. Fiz. **42** (2), 194 (2001).
14. G. P. Epshtein and O. A. Kaibyshev, *High-Strain-Rate Deformation and Structure of Metals* (Metallurgiya, Moscow, 1971) [in Russian].
15. G. V. Garkushin, A. S. Savinykh, G. I. Kanel, S. V. Razorenov, D. Jones, W. G. Proud, and L. R. Botvina, J. Phys.: Conf. Ser. **500**, 112027 (2014).
16. M. A. Meyers and L. E. Murr, *Shock Waves and High-Strain-Rate Phenomena in Metals* (Springer, New York, 1981; Metallurgiya, Moscow, 1984).
17. V. A. Ogorodnikov, E. Yu. Borovkova, and S. V. Erunov, Combust., Explos., Shock Waves **40** (5), 597 (2004).
18. V. D. Gluzman, G. I. Kanel', V. F. Loskutov, V. E. Fortov, and I. E. Khorev, Probl. Prochn. **8**, 52 (1985).
19. G. T. Gray III, N. K. Bourne, M. A. Zocher, P. J. Maudlin, and J. C. F. Millett, in *Shock Compression of Condensed Matter–1999*, Ed. by M. D. Furnish, L. C. Chhabildas, and R. S. Hixson (American Institute of Physics, Woodbury, New York, 2000), p. 509.
20. G. T. Gray III, M. F. Lopez, N. K. Bourne, J. C. F. Millett, and K. C. Vecchio, in *Shock Compression of Condensed Matter–2001*, Ed. by M. D. Furnish, N. N. Thadhani, and Y. Horie (American Institute of Physics, Melville, New York, 2002), p. 479.
21. S. V. Razorenov, G. I. Kanel', G. V. Garkushin, and O. N. Ignatova, Phys. Solid State **54** (4), 790 (2012).
22. G. V. Garkushin, G. I. Kanel', and S. V. Razorenov, Phys. Solid State **54** (5), 1079 (2012).
23. G. I. Kanel, C. V. Razorenov, A. A. Bogatch, A. V. Utkin, V. E. Fortov, and D. E. Grady, J. Appl. Phys. **79** (11), 8310 (1996).
24. G. I. Kanel', S. V. Razorenov, and V. E. Fortov, Sov. Phys. Dokl. **29** (3), 241 (1984).

Translated by O. Borovik-Romanova